ELSEVIER

Ceramics International 27 (2001) 99–104

CERAMICS INTERNATIONAL

www.elsevier.com/locate/ceramint

Effect of Al_2O_3 additions on the crystallization behaviour and bending strength of a Li_2O–ZnO–SiO_2 glass-ceramic

E. Demirkesen *, E. Maytalman

Department of Metallurgical and Materials Engineering, Faculty of Chemical and Metallurgical Engineering, Istanbul Technical University, 80626 Maslak, Istanbul, Turkey

Received 12 December 1999; received in revised form 19 January 2000; accepted 8 March 2000

Abstract

In this study, the effect of partial replacement of ZnO by Al_2O_3 on the crystallization behaviour and bending strength of a Li_2O–ZnO–SiO_2 glass-ceramic was investigated using differential thermal analysis (DTA), X-ray diffraction (XRD), scanning electron microscopy (SEM), and mechanical property. The crystallization sequence of the glasses was determined by XRD analysis of the samples subjected to isothermal and nonisothermal heat treatments. All compositions showed volume crystallization with rather fine microstructures. The maximum bending strength was obtained for composition containing 4 wt.% Al_2O_3, above which a marked decrease was determined. The changes in phase assemblage and microstructures depended on the alumina content and applied heat treatments; these were correlated to the strength of the glass-ceramics.

Keywords: D. Glass; D. Glass-ceramic; Crystallization

1. Introduction

Glass-ceramics derived from the Li_2O–ZnO–SiO_2 system may contain other oxides such as K_2O, Na_2O, B_2O_3, and Al_2O_3. Minor constituents may have important effects on glass forming ability of the batch, on its crystallization behaviour, and on the tendency to phase separation during casting or reheating of the glass. Also, they may alter the type and amount of the phases crystallized which in turn may change properties of the product. P_2O_5 is a common and effective nucleating agent for this system [1]. Stable and metastable phase relations in the Li_2O–ZnO–SiO_2 system were examined by West and Glasser [2,3]. Depending on the composition, lithium disilicate, lithium metasilicate, lithium zinc silicate, and silica can be present as being major phases in this type of glass-ceramics. These phases are characterized by their high or moderately high thermal expansion coefficients making the glass-ceramic suitable for seals. Also, glass-ceramics containing lithium disilicate and silica as being major phases possess high mechanical strength. Crystallization behaviour and properties of the Li_2O–ZnO–SiO_2 system, in particular containing low ZnO contents, were studied by many authors [4–10]. The effect of alumina additions, however, were examined for only a few complex compositions [11–13].

The purpose of this research was to investigate the effect of Al_2O_3, substituted for ZnO up to 11 wt.%, on the crystallization behaviour and bending strength of a lithium zinc silicate glass-ceramic; the weight percentage of other constituents was kept constant.

2. Experimental procedures

The effects of alumina substitutions were examined by preparing glasses containing 0, 4, 6, 8, and 11 wt.% Al_2O_3 (Table 1). 3 wt.% P_2O_5 was used as nucleating agent for all compositions studied. In addition, for the composition containing 11 wt.% Al_2O_3, the nucleating efficiency of P_2O_5 (A11P3 glass) was compared with that of TiO_2 at 3 and 5 wt.% (A11T3 and A11T5 glasses). The resulting microstructures of these compositions were also compared with those obtained without nucleating agents (A11 glass). Merck quality Al_2O_3, ZnO, H_2SiO_3, Li_2CO_3, P_2O_5, and TiO_2 were used as raw materials. A mechanical mixture of the starting materials, giving a

* Corresponding author. Fax: +90-212-285-3512.
E-mail address: edemir@itu.edu.tr (E. Demirkesen).

0272-8842/01/$20.00
PII: S0272-8842(00)00048-1

Table 1
Nominal compositions of the glasses (wt.%)

Glass code	Li_2O	ZnO	Al_2O_3	SiO_2	P_2O_5	TiO_2
A0	10	32	–	55	3	–
A4	10	28	4	55	3	–
A6	10	26	6	55	3	–
A8	10	24	8	55	3	–
A11P3	10	21	11	55	3	–
A11T3	10	21	11	55	–	3
A11T5	9.79	20.56	10.77	53.86	–	5
A11	10.31	21.65	11.34	56.70	–	–

100 g batch, was prereacted in a Pt crucible at about 950°C for 4 h and then melted at 1400 to 1450°C for 4 h. To achieve a good homogenity, the melts were poured into distilled water and after drying and grinding were remelted. After repeating this procedure twice, the melts were refined for 14–16 h and cast into preheated graphite molds. Glass transition and crystallization temperatures of the bulk glass samples (2.5–3 mm) were determined by differential thermal analyses (DTA) with a heating rate of 10°C min^{-1} (Netzch, α-alumina reference material). Crystallization heat treatments were planned according to the DTA results. Crystalline phases developed during isothermal or nonisothermal heating were determined by X-ray diffraction (XRD) using a diffractometer (Philips PW1820) employing CoK_α, for $2\theta = 15$–$90°$. Samples subjected to isothermal treatments were polished and then etching with 5% HF solution for 20–30 s, coated with gold and examined by scanning electron microscopy (Jeol JSM-330). Mechanical strength of the samples was determined at room temperature by three point bending test using an Instron testing machine operating at a cross-head speed of 0.5 mm min^{-1}. Four specimens having 7 mm diameter and 60 mm length were used for each strength determination.

3. Results and discussions

3.1. Glass formation ability of the batches, DTA and XRD results

Homogeneous, transparent glasses were obtained from all compositions studied without showing any tendency to uncontrolled devitrification on cooling in the preheated molds. Refining of the melts needed higher temperatures and longer times as the alumina content increased. This behaviour can be attributed to the increase of the melt viscosity with increasing alumina content. For a composition containing 11 wt.% Al_2O_3, fluidity and refining properties of the melt could be markedly improved by using 5 wt.% TiO_2. Because of its high viscosity at 1450°C, bubble-free bending samples could not be obtained from the composition A11 containing neither P_2O_5 nor TiO_2. Small samples prepared from this composition, however, were almost bubble free and were used for microstructure examinations.

DTA results of the nucleated glasses are given in Table 2. As can be seen, the glass transition and the first crystallization temperature of the original alumina free glass increase gradually with alumina additions. This behaviour can be attributed to strengthening of the bonds within the glass network upon replacement of ZnO by Al_2O_3.

Crystallization sequence of the alumina free composition, A0, is quite simple, and consists of two steps; precipitation of a lithium zincsilicate phase in the early stage of crystallization with a composition close to $Li_3Zn_{0.5}SiO_4$ (γ_{II}-LZS, JCPDS card no. 24-685), and the crystallization of cristobalite at higher temperatures. Thus, the first and the second exothermic heat effects represent these crystallization stages, respectively. For the alumina-containing compositions, crystallization of γ_{II}-LZS at the first exothermic peak temperatures is followed by that of a lithium aluminosilicate$_{ss}$ (solid solution) upon heating to the second peak temperatures (Fig. 1). The composition of this solid solution changes gradually from $Li_xAl_xSi_{3-x}O_6$ (JCPDS card no. 31-707) to $Li_xAl_xSi_{1-x}O_2$ (virgilite, JCPDS card no. 40-73) as the substituted alumina content is increased. For composition A4, the lithium aluminosilicate$_{ss}$ transforms firstly to a β-quartz$_{ss}$, which has intensive XRD lines at 3.38, 4.33 and 1.85 Å, upon heating to the third peak temperature. These d spacings are very close to 3.38, 4.34, 1.84 Å reported for "impure silica" (JCPDS card no. 12-708) having a composition located at the silica rich end of the SiO_2–$LiAlSiO_4$ join and can be compared with the values 3.40, 4.34, 1.84 Å given for β-quartz (JCPDS card no. 11-252). The β-quartz$_{ss}$, once formed, persists as a metastable phase at temperatures between 850 and 920°C above which β-spodumene (β-$Li_2O.Al_2O_3.4SiO_2$) begins to precipitate while a slight shift occurs in the d spacings of the β-quartz$_{ss}$. For composition A6, the lithium aluminosilicate$_{ss}$ transforms to a mixture of β-spodumene$_{ss}$ and impure silica at the third peak

Table 2
DTA results for the nucleated glasses (°C)[a]

Glass code	T_g	T_{p1}	T_{p2}	T_{p3}
A0	500	647	891	–
A4	502	653	791	848
A6	510	665	762	804
A8	513	674	757	791
A11P3	523	715	787	900
A11T3	521	705	868	–
A11T5	530	640	750	823
A11	517	699	752	797

[a] T_g = glass transition temperature (dip point); T_{p1}, T_{p2}, T_{p3} = first, second and third crystallization temperatures, respectively.

temperature. As seen from Fig. 1b, the impure silica formed goes into the β-spodumene structure upon heating above 900°C but begins to precipitate again as a minor phase when the glass-ceramic was cooled at ~1°C min^{-1}. For glasses containing 8 and 11 wt.% Al_2O_3, the transformation of virgilite to β-spodumene$_{ss}$ occurs at the third peak temperature without precipitation of silica. As seen from Table 2, A11T3 glass has two exothermic peaks both in the as-cast and nucleated states, the first of which is due to the coprecipitation of γ_{II}-LZS and virgilite while the second corresponds to the transformation of virgilite to β-spodumene$_{ss}$. The γ_{II}-LZS formed in all compositions in the early stages of crystallization was found to transform to γ_0-Li_2ZnSiO_4 (γ_0-LZS) at higher temperatures and remained in this form upon cooling to room temperature.

3.2. Microstructures and bending strengths

Volume crystallization with rather fine microstructures was observed for all compositions studied. Examples of the SEM micrographs are given in Fig. 2. XRD analysis of these samples showed that one of the two microstructure constituents was γ_0-LZS for all compositions, and the second was cristobalite for A0, β-quartz$_{ss}$ (impure silica) for A4, and β-spodumene$_{ss}$ for the other glass-ceramics. As can be seen from the micrographs, the interconnected microstructure of A0 glass-ceramic is modified and becomes relatively coarser with alumina additions of above 4 wt.%, leading the formation of β-spodumene$_{ss}$. On the other hand, close similarities between the microstructure of nucleating agent free A11 composition and those of A11P3,

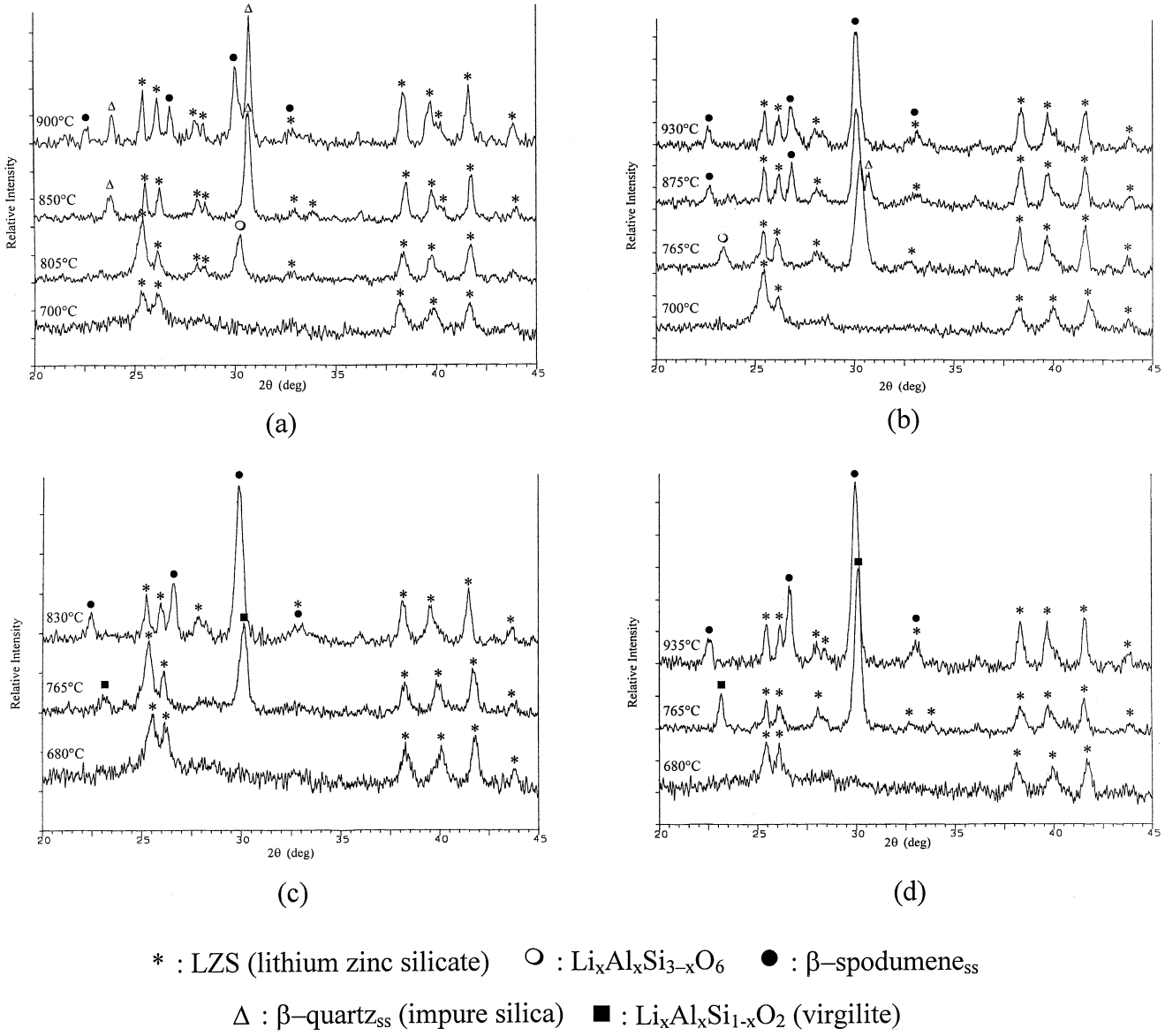

Fig. 1. XRD powder patterns of glasses held at different temperatures for 1 h: (a) A4, (b) A6, (c) A8, (d) A11P3.

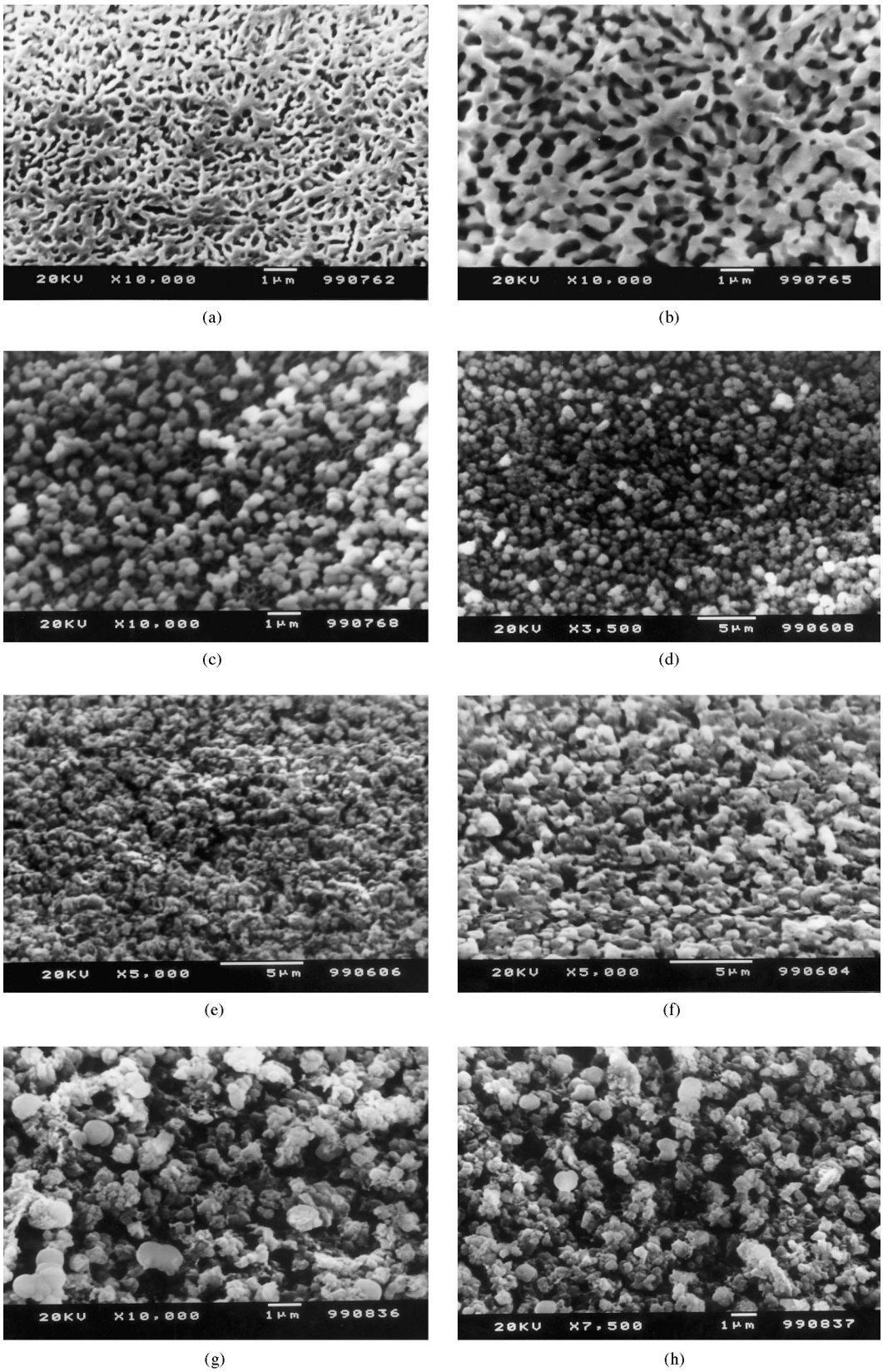

Fig. 2. Microstructures of glass-ceramics developed at conditions giving the highest bending strength: (a) A0, (b) A4, (c) A6, (d) A8, (e) A11T5, (f) A11T3, (g) A11P3, (h) A11 (540°C/1 h + 875°C/3 h).

Table 3
Bending strength of glasses and glass-ceramics

Glass code	Applied heat treatments (°C/h)	Crystallized phases[a]	Bending strength (MPa)	
			Glass	Glass-ceramic
A0	500/1	Amorphous	137±6	
	520/1 + 800/2 + 920/1	γ_0-LZS + cr		70±8
	520/1 + 670/2 + 850/2	γ_0-LZS + cr		88±5
	520/1 + 920/3	γ_0-LZS + cr		55±7
A4	500/1	Amorphous	123±4	
	520/1 + 875/3	γ_0-LZS + β-Q_{ss}		290±4
	520/1 + 840/2 + 900/1	γ_0-LZS + β-Q_{ss} + β-spo_{ss}		232±9
A6	510/1	Amorphous	135±6	
	530/1 + 840/2 + 900/1	γ_0-LZS + β-Q_{ss} + β-spo_{ss}		175±10
A8	510/1	Amorphous	124±5	
	530/1 + 825/3	γ_0-LZS + β-spo_{ss}		166±9
A11T5	530/1	Amorphous	145±2	
	550/1 + 860/3	γ_0-LZS + β-spo_{ss}		170±7
A11T3	520/1	Amorphous	138±8	
	540/1 + 875/3	γ_0-LZS + β-spo_{ss}		119±9
A11P3	520/1	Amorphous	134±6	
	540/1 + 875/3	γ_0-LZS + β-spo_{ss}		128±7

[a] γ_0-LZS, γ_0-Li_2ZnSiO_4; cr, cristobalite; β-Q_{ss}, β-$quartz_{ss}$; β-spo_{ss}, β-$spodumene_{ss}$.

A11T3, and A11T5 makes it difficult to decide wheather the nucleating agents used or a possible homogeneous nucleation plays predominant role on the microstructures developed. The high viscosity of A11 glass can also hinder excess grain growth.

The bending strengths of the annealed glasses and their glass-ceramics are given in Table 3 together with the applied heat treatments and the resultant crystalline phases. Bending strength of the original alumina free glass seems not to be affected markedly by alumina additions. As seen from Table 3, the strength of A0 glass-ceramic is lower than that of its glass by a factor of ~2. Glass-ceramics having lithium zinc silicate and cristobalite phases can be expected normally to have higher strength than those of determined. Microcracks observed at the LZS-glass grain boundaries before the precipitation of cristobalite suggests that the high thermal stresses induced by the mismatch in the thermal expansion coefficient between the high expansion LZS and that of Li^+ and Zn^{2+} depleted glass may be responsible for the low strength. A4 glass-ceramic, on the other hand, showed the highest strength among the compositions studied when it was crystallized at 875°C for 3 h resulting in crystallization of γ_0-LZS and impure silica. Its strength was reduced from 290 to 232 MPa when the crystallization temperature was increased to 900°C causing β-$spodumene_{ss}$ to precipitate as a minor phase. A marked decrease in the strength occurred when the amount of alumina content exceeded 4 wt.%. The maximum strengths that could be achieved for compositions A6, A8, and A11T5 were 175, 166, and 170 MPa, respectively. An important factor that can be responsible for the decrease in the strength is the coexistence of low and high expansion phases in these glass-ceramics (and also in A4 glass-ceramic crystallized at 900°C). Thermal expansion coefficient of pure β-spodumene (1:1:4) is 9×10^{-7}, while those of 1:1:6, 1:1:8 and 1:1:10 solid solutions are lower: 5×10^{-7}, 3×10^{-7}, and 5×10^{-7} C^{-1}, respectively [1]. The directional expansion coefficient of γ_0-LZS, on the other hand, is 160×10^{-7}, 110×10^{-7}, $180\times10^{-7}°C^{-1}$ (25–1030°C) for the axes *a*, *b*, and *c*, respectively [3]. High internal stresses caused by these mismatches in the thermal expansion coefficients can be expected to reduce the strength of the glass-ceramics. In addition, relatively coarsening of the microstructure with increasing alumina content, and the formation of β-$spodumene_{ss}$ instead of impure silica, which has a lower strength than that of the latter, can have an additional effect on the weakening of the glass-ceramics. Further decrease in the strengths of A11P3 and A11T3 compositions may be due to the possible presence of micron-sized gas voids formed in the glass melts which have lower fluidity than A11T5.

4. Conclusions

With the partial replacement of ZnO by Al_2O_3 up to 11 wt.%, it is possible to obtain glass forming melts having satisfactory fluidty at temperatures between 1350 and 1450°C from which glass-ceramics showing volume crystallization with fairly fine microstructures can be produced. 3 wt.% P_2O_5 for compositions containing up

to 8 wt.% Al_2O_3, or 5 wt.% TiO_2 for composition containing 11 wt.% Al_2O_3 was found to have suitable fluxing and nucleating effects. For the applications where high strength is required, glass-ceramic containing 4 wt.% Al_2O_3 seems to be a suitable material having a bending strength of 290 MPa. Glass-ceramics having alumina content in the range of 6 to 11 wt.%, on the other hand, have lower bending strengths (166 to 175 MPa), but can be expected to have higher thermal shock resistance and higher chemical stability because of the presence of β-spodumene phase having these properties.

References

[1] P.W. McMillan, Glass-Ceramics, 2nd Edition, Academic Press, London, New York, San Francisco, 1979, pp. 95–96, 165–166, 228.
[2] A.R. West, F.P. Glasser, Crystallisation of lithium zinc silicates. Part 1, Phase equilibria in the system Li_4SiO_4–Zn_2SiO_4, J. Mater. Sci. 5 (1970) 557–565.
[3] A.R. West, F.P. Glasser, Crystallization of lithium zinc silicates. Part 2, Comparison of the metastable and stable phase relations and the properties of the lithium zinc ortosilicates, J. Mater. Sci. 5 (1970) 676–688.
[4] Z.X. Chen, P.W. McMillan, Crystallization behaviour of a high zinc content Li_2O–ZnO–SiO_2 glass-ceramic and the effect of K_2O additions, J. Am. Ceram. Soc. 68 (4) (1985) 220–224.
[5] I.W. Donald, B.L. Metcalfe, D.J. Wood, J.R. Copley, The preparation and properties of some lithium zinc silicate glass-ceramics, J. Mater. Sci. 24 (1989) 3892–3903.
[6] I.W. Donald, B.L. Metcalfe, A.E.P. Morris, Influence of transition metal oxide additions on the crystallization kinetics, microstructures and thermal expansion characteristics of a lithium zinc silicate glass, J. Mater. Sci. 27 (1992) 2979–2999.
[7] R. Morrell, K.H.G. Ashbee, High temperature creep of lithium zinc silicate glass-ceramics. Part 1, General behaviour and creep mechanisms, J. Mater. Sci. 8 (1973) 1253–1270.
[8] R. Morrell, K.H.G. Ashbee, High temperature creep of lithium zinc silicate glass-ceramics. Part 2, Compression creep and recovery, J. Mater. Sci. 8 (1973) 1271–1277.
[9] R. Lyall, K.H.G. Ashbee, High temperature plasticity of lithium zinc silicate glass-ceramics. Part 1, Constant strain-rate tests, J. Mater. Sci. 9 (1979) 576–582.
[10] R. Lyall, K. James, K.H.G. Ashbee, High temperature plasticity of lithium zinc silicate glass-ceramics. Part 2, A model based on dilatancy and stress-induced dissolution, J. Mater. Sci. 9 (1979) 583–590.
[11] A.A. Omar, A.W.A. El-Shennavi, A.R. El-Ghannam, Thermal expansion of Li_2O–ZnO–Al_2O_3–SiO_2 glasses and corresponding glass-ceramics, J. Mater. Sci. 26 (1991) 6049–6056.
[12] C. Wang, W. Xu, Study of crystallization of the Li_2O–ZnO–Al_2O_3–SiO_2 system glasses, J. Non-Cryst. Solids 80 (1986) 237–242.
[13] M.J. Fairweather, J.A. Topping, M.K. Murthy, Effect of Al_2O_3 on a complex Li_2O–ZnO–SiO_2 glass-ceramic, J. Am. Ceram. Soc. 58 (5–6) (1975) 260.